PMILACG Model: A Predictive Model for Identifying Invasiveness of Lung Adenocarcinoma Based on High-Resolution CT-Determined Ground Glass Nodule Features

Bo Yan,[1,2] Yifeng Jiang,[3] Shijie Fu[4] and Rong Li[1,2]

[1]Clinical Research Unit, Shanghai Chest Hospital, School of Medicine, Shanghai Jiao Tong University, Shanghai, China
[2]Department of Pulmonary Medicine, Shanghai Chest Hospital, Shanghai Jiao Tong University, Shanghai, China
[3]Department of Radiology, Shanghai Chest Hospital, Shanghai Jiao Tong University, Shanghai, China
[4]Department of Thoracic Surgery, Shanghai Chest Hospital, School of Medicine, Shanghai Jiao Tong University, Shanghai, China

The morphology of ground-glass nodule (GGN) under high-resolution computed tomography (HRCT) has been suggested to indicate different histological subtypes of lung adenocarcinoma (LUAD); however, existing studies only include the limited number of GGN characteristics, which lacks a systematic model for predicting invasive LUAD. This study aimed to construct a predictive model based on GGN features under HRCT for LUAD. A total of 1,189 surgical LUAD patients were enrolled, and their GGN-related features were assessed by 2 individual radiologists. The pathological diagnosis of the invasive LUAD was established by pathologic examination following surgery (including 1,073 invasive and 526 non-invasive LUAD). After adjustment by multivariate logistic regression, GGN diameter (OR = 1.382, 95% CI: 1.300-1.469), mean CT attenuation (OR = 1.007, 95% CI: 1.006-1.009), heterogeneous uniformity of density (OR = 2.151, 95% CI: 1.587-2.915), not defined nodule-lung interface (OR = 1.915, 95% CI: 1.384-2.651), GGN with spiculation (OR = 2.097, 95% CI: 1.519-2.896), type I (OR = 1.678, 95% CI: 1.216-2.371), and type II (OR = 3.577, 95% CI: 1.153-11.097) vessel changes were independent risk factors for invasive LUAD. In addition, a predictive model integrating these six independent GGN features was established (named as invasion of lung adenocarcinoma by GGN features (ILAG)), and receiver-operating characteristic curve illustrated that the ILAG model presented good predictive value for invasive LUAD (AUC: 0.905, 95% CI: 0.890-0.919). In conclusion, The ILAG predictive model, which integrates imaging features of GGN via HRCT, including diameter, mean CT attenuation, heterogeneous uniformity of density, not defined nodule-lung interface, GGN with spiculation, type I, and type II vessel changes, shows great potential for early estimation of LUAD invasiveness.

Introduction

Lung cancer is the most prevalent malignancy in Chinese population, among whose histological subtypes, lung adenocarcinoma (LUAD) accounts for 40% of all lung cancer cases (Adams et al. 2023; Lv et al. 2023; Sathish et al. 2024). The pathological diagnosis divides lung adeno-carcinoma into atypical adenomatous hyperplasia (AAH), adenocarcinoma in situ (AIS), minimally invasive adeno-carcinoma (MIA), invasive adenocarcinoma (IAC), in which the former two are non-invasive and the latter two are invasive (Travis et al. 2011). Clinically, the invasive-ness of LUAD not only forecasts the prognosis but also instructs treatment, for instance, limited resection is pre-

ferred for non-invasive cases to preserve lung function, and invasive cases require thoracopic wedge resection, segmental or sub-segmental resection with intensive monitoring (Mangiameli et al. 2022; Udelsman and Blasberg 2023). Currently, the determination of LUAD invasiveness relies on the histopathological diagnosis from the resected tumor tissues via surgery, however, the awaiting during operation is under high risk of losing the best treatment opportunity, in addition, the adverse reactions of surgery also worsen the prognosis (Ni et al. 2020; Godoy et al. 2022). Therefore, a pre-operational determination of tumor invasiveness is necessary for timely and appropriate treatment for lung adenocarcinoma.

Ground-glass nodule (GGN) refers to increased density and focal cloudy density shadows with clear vessels and bronchus by high resolution computed tomography (HRCT) imaging (Liang et al. 2024; Lung Cancer Medical Education Committee of the Chinese Medical Education et al. 2024; Wang et al. 2024). The existence of GGN indicates malignant progression risk of lesion in lung, and the morphology of GGN has been suggested to indicate different histological subtypes of LUAD in some guidelines to assist subsequent management (Gould et al. 2013; Bai et al. 2016; MacMahon et al. 2017). In addition, the HRCT characteristics of GGN has been studied to predict invasiveness of LUAD, for example, the shape, size, attenuation as well as proportion of solid components of GGN are correlated with the likelihood of invasive LUAD (Lee et al. 2013; Mei et al. 2018; Chu et al. 2020). However, existing studies only include limited number of GGN characteristics, which lack comprehensiveness, and there also lack a systematic model for predicting invasive LUAD. Therefore, we assessed the GGN features (including: location, distance from pleura, diameter, area, mean CT value, uniformity of density, shape, nodule-lung interface, spiculation, pleural indentation, air bronchogram, vacuole sign, vessel changes, and lobulation) via HRCT and established a predictive model named "invasion of lung adenocarcinoma (ILAG) by GGN features" for invasiveness of LUAD.

Methods

Patients

This retrospective study respectively analyzed the HRCT data of 1,189 LUAD patients with 1,599 HRCT-confirmed pure-GGN or part-solid nodule, who underwent surgery in the Shanghai Chest Hospital between May 2020 and November 2021. The eligible patients satisfied following inclusion criteria: (a) presence of GGN on HRCT images before surgery; (b) pathological diagnosis of LUAD including AAH, AIS, MIA, or IAC, which was in accordance with the classification criteria proposed by World Health Organization (WHO) 2015 (Travis et al. 2015); (c) time interval between HRCT and surgery < 1 month; (d) HRCT features data were available. Patients with one of the following conditions were not included in the analysis: (a) there were motion artifacts on HRCT images which

could hamper accurate assessment; (b) there were diffuse lesions distributed around the GGN; (c) there was distant metastasis. Ethics Committee of Shanghai Chest Hospital, Shanghai Jiao Tong University had given ethical approval for the study, and the included patients provided the written informed consents.

HRCT screening

A Philips iCT 256 scanner (Brilliance, Philips, USA) was used for generating the CT scans. Initially, FOV of 400 mm, section thickness and interval of 1.0 and 1.0 mm, and window setting with the level of –520 and width of 1,450, respectively, were applied for the routine CT scans. To identify the specific lung nodules, the following parameters were set for the target scans: 0.6-0.8 second scan time; matrix, $1,024 \times 1,024$; FOV, 140 mm; 120 kVp; and 250 mA; window setting with the level of –520 and width of 1,450. The reconstruction algorithms for the routine and target HRCT scans were referred to the previous study (Zhang et al. 2016).

GGN features and definitions

HRCT imaging data were reviewed by 2 radiologists with more than 10 years of experience. If the judgments of the two radiologists were different, then, a third investigator would be invited to make the final decision. The following 15 GGN-related features were collected (Shao et al. 2019): (a) Location: right upper lobe, right middle lobe, right lower lobe, left upper lobe, left lower lobe; (b) Distance from pleura: ≥ 2 mm or < 2 mm; (c) Diameter (by manually): the largest diameter of GGN; (d) Area (measured by MIDS-PNAS (version 1.3.0.1) (Beijing Deepwise Science and Technology Co., Ltd., China)): the largest area of GGN on axial CT images; (e) Mean CT value (measured by MIDS-PNAS (version 1.3.0.1) (Beijing Deepwise Science and Technology Co., Ltd., China): mean CT attenuation of GGN; (f) Uniformity of density: homogeneous or heterogeneous; (g) Shape: round/oval or Irregular; (h) Margin status: smooth or coarse; (i) Nodule-lung interface: well defined or not defined; (j) Spiculation: yes or no; (k) Pleural indentation: yes or no; (l) Air bronchogram: yes or no; (m) Vacuole sign: yes or no; (n) Vessel changes: no: without vessel change; type I: vessels crossing nodules; type II: distorted or dilated vessels detected within nodules; type III: lesion vessels were dilated and distorted or there was more complicated vasculature than described in types I and II; (o) Lobulation: yes or no. The specific GGN features were shown in the Supplementary Fig. S1A-J.

Pathological diagnosis and classification

Pathological diagnosis was established by pathologic examination following surgery. There were 63 AAH, 463 AIS, 554 MIA, and 519 IAC among 1,599 LUAD in the study. According to the 2015 WHO classification criteria of lung tumors (Travis et al. 2015), 1,599 LUAD were classified into two groups: non-invasive LUAD (n = 526) includ-

ing AAH and AIS; invasive LUAD (n = 1,073) including MIA and IAC.

Statistical analysis

Statistical analysis was carried out using SPSS 26.0 software (IBM, Chicago, Illinois, USA), and graph drawing was completed suing GraphPad Prism 9.01 (GraphPad Software Inc., San Diego, California, USA). Qualitative data were described as number with percentage [No. (%)], and quantitative data were described as mean with standard deviation (SD) or median with interquartile range (IQR) according to the normality determined by Kolmogorov-Smirnov(K) test. Comparison between two groups was determined by Chi-square test (or Fisher's exact test), Student's t test or Wilcoxon rank sum test. Univariate and forward stepwise-multivariate logistic regression analysis was used to analyze factors associated with invasive LUAD (vs. non-invasive) and to construct ILAG predictive model. Receiver-operating characteristic (ROC) curve and the area under the ROC curve (AUC) were applied to evaluate the predictive performance of the ILAG model for invasive LUAD risk. The nomogram was used to estimate the risk of invasive LUAD. Statistical significance was set as P value less than 0.05.

Results

Clinical characteristics and GGN features of LUAD patients

The total LUAD patients were at mean age of 55.2 ± 12.1 years and 69.5%/30.5% of them were females/males (Supplementary Table S1). The demographic characteristics between non-invasive LUAD and invasive LUAD patients differed, with elder age ($P < 0.001$) and lower proportion of females ($P = 0.032$) in invasive LUAD compared with non-invasive LUAD patients. There were 526 non-invasive and 1,073 invasive LUAD by pathological confirmation respectively. Among the GGN features, only the GGN location was similar between invasive LUAD and non-invasive LUAD; while the distance from pleura was shorter, median diameter, area and mean CT attenuation was larger, heterogeneous density, irregular shape, coarse margin, not defined nodule-lung interface, spiculation, pleural indentation, air bronchogram, vacule sign, Type II and Type III vessel change and lobulation were more frequent in invasive LUAD compared with non-invasive LUAD (all $P < 0.05$). The detailed GGN features were shown in Table 1. Besides, the representative radiological images of different GGN features were shown in Supplementary Fig. S1.

GGN features contributing to invasive LUAD

GGN features are closely correlated with invasive LUAD. GGN features including: distance from pleura (< 2 mm vs. ≥ 2 mm), diameter, area, mean CT attenuation, uniformity of density (heterogeneous vs. homogeneous), shape (irregular vs. round or oval), margin status (coarse vs. smooth), nodule-lung interface (not defined vs. well

defined), with spiculation (yes vs. no), with pleural indentation (yes vs. no), with air bronchogram (yes vs. no), with vacuole sign (yes vs. no), with vessel changes (type I and type II vs. no), with lobulation (yes vs. no) contributed to invasive LUAD (all $P < 0.05$) (Table 2).

Independent GGN features for invasive LUAD

All GGN features were included in multivariate logistic regression model analysis. Among the factors contributing to invasive LUAD, GGN diameter ($P < 0.001$), mean CT attenuation ($P < 0.001$), heterogeneous uniformity of density ($P < 0.001$), not defined nodule-lung interface ($P < 0.001$), GGN with spiculation ($P < 0.001$), type I ($P = 0.002$), and type II ($P = 0.027$) vessel changes were independent risk factors for invasive LUAD (Table 3).

ILAG model for invasive LUAD risk

The predictive performances of six independent GGN features as well as the ILAG model integrating the six features for invasive LUAD were assessed by ROC analysis. GGN diameter (AUC: 0.843, 95% CI: 0.824-0.863) (Fig. 1A), GGN mean CT attenuation (AUC: 0.725, 95% CI: 0.700-0.751) (Fig. 1B), GGN uniformity of density (AUC: 0.749, 95% CI: 0.722-0.775) (Fig. 1C), nodule-lung interface (AUC: 0.631, 95% CI: 0.601-0.661) (Fig. 1D), GGN with spiculation (AUC: 0.724, 95% CI: 0.698-0.750) (Fig. 1E), GGN with vessel changes (AUC: 0.716, 95% CI: 0.690-0.743) (Fig. 1F), were of relatively good value in telling invasive LUAD from non-invasive LUAD, and the ILAG model integrating the six independent GGN features presented even better predictive value in distinguishing invasive LUAD from non-invasive LUAD (AUC: 0.905, 95% CI: 0.890-0.919) (Fig. 1G). The detail equation for this predictive model was as follows: P = Exp [–1.098 + 0.323 (GGN diameter) + 0.007 (GGN CT attenuation) + 0.766 (GGN uniformity of density) + 0.650 (Nodule-lung interface) + 0.741 (GGN with spiculation) + 0.518 (GGN with Type I vessel changes) + 1.275 (GGN with Type II vessel changes) + 15.348 (GGN with Type III vessel changes)]/1 + Exp [–1.098 + 0.323 (GGN diameter) + 0.007 (GGN CT attenuation) + 0.766 (GGN uniformity of density) + 0.650 (Nodule-lung interface) + 0.741 (GGN with spiculation) + 0.518 (GGN with Type I vessel changes) + 1.275 (GGN with Type II vessel changes) + 15.348 (GGN with Type III vessel changes)]. In addition, a nomogram model was also established for indicating the LUAD risk (Supplementary Fig. S2).

Subgroup analyses

For subgroup analyses, in non-invasive LUAD subtypes, most GGN features were similar; however, GGN diameter, area, well defined nodule-lung interface, type I, and type II vessel changes were higher in AIS compared with AAH (all $P < 0.05$) (Supplementary Table S2), whereas in invasive LUAD subtypes, most GGN features were different, but GGN location was similar between MIA

Table 1. Clinical features of GGN in LUAD patients.

Items	Total (N = 1599)	Non-invasive LUAD (n = 526)	Invasive LUAD (n = 1073)	P value
Pathological classification				
AAH, No. (%)	63 (3.9)	63 (12.0)	0 (0.0)	-
AIS, No. (%)	463 (29.0)	463 (88.0)	0 (0.0)	-
MIA, No. (%)	554 (34.6)	0 (0.0)	554 (51.6)	-
IAC, No. (%)	519 (32.5)	0 (0.0)	519 (48.4)	-
GGN features				
Location, No. (%)				0.591
Right upper lobe	547 (34.2)	180 (34.2)	367 (34.2)	
Right lower lobe	297 (18.6)	107 (20.3)	190 (17.7)	
Right middle lobe	151 (9.4)	52 (9.9)	99 (9.2)	
Left upper lobe	410 (25.6)	124 (23.6)	286 (26.7)	
Left lower lobe	194 (12.1)	63 (12.0)	131 (12.2)	
Distance from pleura, No. (%)				< 0.001
≥ 2 mm	942 (58.9)	356 (67.7)	586 (54.6)	
< 2 mm	657 (41.1)	170 (32.3)	487 (45.4)	
Diameter (mm), median (IQR)	9.8 (7.3-13.5)	7.0 (5.8-8.7)	11.6 (8.9-15.6)	< 0.001
Area (mm^2), median (IQR)	59.9 (35.5-108.7)	34.4 (23.5-49.2)	83.9 (50.9-140.9)	< 0.001
Mean CT attenuation (HU), mean ± SD	−573.2 ± 122.6	−635.2 ± 101.2	−542.8 ± 120.8	< 0.001
Uniformity of density, No. (%)				< 0.001
Homogeneous	561 (35.1)	360 (68.4)	201 (18.7)	
Heterogeneous	1038 (64.9)	166 (31.6)	872 (81.3)	
Shape, No. (%)				< 0.001
Round or oval	591 (37.0)	301 (57.2)	290 (27.0)	
Irregular	1008 (63.0)	225 (42.8)	783 (73.0)	
Margin status, No. (%)				< 0.001
Smooth	382 (23.9)	228 (43.3)	154 (14.4)	
Coarse	1217 (76.1)	298 (56.7)	919 (85.6)	
Nodule-lung interface, No. (%)				< 0.001
Well defined	466 (29.1)	246 (46.8)	220 (20.5)	
Not defined	1133 (70.9)	280 (53.2)	853 (79.5)	
Spiculation, No. (%)				< 0.001
No	811 (50.7)	425 (80.8)	687 (64.0)	
Yes	788 (49.3)	101 (19.2)	386 (36.0)	
Pleural indentation, No. (%)				< 0.001
No	1212 (75.8)	476 (90.5)	736 (68.6)	
Yes	387 (24.2)	50 (9.5)	337 (31.4)	
Air bronchogram, No. (%)				< 0.001
No	1495 (93.5)	518 (98.5)	977 (91.1)	
Yes	104 (6.5)	8 (1.5)	96 (8.9)	
Vacuole sign, No. (%)				< 0.001
No	1320 (82.6)	480 (91.3)	840 (78.3)	
Yes	279 (17.4)	46 (8.7)	233 (21.7)	
Vessel changes, No. (%)				< 0.001
No	429 (26.8)	272 (51.7)	157 (14.6)	
Type I	1009 (63.1)	249 (47.3)	760 (70.8)	
Type II	156 (9.8)	5 (1.0)	151 (14.1)	
Type III	5 (0.3)	0 (0.0)	5 (0.5)	
Lobulation, No. (%)				< 0.001
No	1306 (81.7)	486 (92.4)	820 (76.4)	
Yes	293 (18.3)	40 (7.6)	253 (23.6)	

Comparison was determinized by Student's t test, Chi-square test, Fisher's exact test, or Wilcoxon rank sum test. LUAD, lung adenocarcinoma; AAH, atypical adenomatous hyperplasia; AIS, adenocarcinoma in situ; MIA, minimally invasive adenocarcinoma; IAC, invasive adenocarcinoma; GGN, ground glass nodule; IQR, interquartile range; CT, computerized tomography; SD, standard deviation.

Table 2. Factors related to invasive LUAD.

Items	Univariate logistic regression model			
			95%CI	
	P value	OR	Lower	Higher
GGN Location				
Right upper lobe	Reference	-	-	-
Right lower lobe	0.361	0.871	0.647	1.172
Right middle lobe	0.724	0.934	0.638	1.366
Left upper lobe	0.381	1.131	0.858	1.491
Left lower lobe	0.912	1.020	0.719	1.446
GGN distance from pleura (< 2 mm vs. ≥ 2 mm)	< 0.001	1.740	1.398	2.166
GGN diameter	< 0.001	1.558	1.480	1.639
GGN area	< 0.001	1.038	1.033	1.043
GGN mean CT attenuation	< 0.001	1.008	1.006	1.009
GGN uniformity of density (heterogeneous vs. homogeneous)	< 0.001	9.408	7.405	11.954
GGN shape (irregular vs. round or oval)	< 0.001	3.612	2.901	4.497
GGN margin status (coarse vs. smooth)	< 0.001	4.566	3.582	5.819
Nodule-lung interface (not defined vs. well defined)	< 0.001	3.406	2.716	4.272
GGN with spiculation (yes vs. no)	< 0.001	7.489	5.831	9.619
GGN with pleural indentation (yes vs. no)	< 0.001	4.359	3.170	5.995
GGN with air bronchogram (yes vs. no)	< 0.001	6.362	3.069	13.190
GGN with vacuole sign (yes vs. no)	< 0.001	2.894	2.069	4.048
GGN with vessel changes				
No	Reference	-	-	-
Type I	< 0.001	5.288	4.147	6.743
Type II	< 0.001	52.321	21.012	130.284
Type III	0.999	-	-	-
GGN with lobulation (yes vs. no)	< 0.001	3.749	2.637	5.330

LUAD, lung adenocarcinoma; OR, odds ratio; CI, confidence interval; GGN, ground glass nodule; CT, computerized tomography.

Table 3. Independent predictors for invasive LUAD.

Items	Multivariate logistic regression model			
			95%CI	
	P value	OR	Lower	Higher
GGN diameter	< 0.001	1.382	1.300	1.469
GGN mean CT attenuation	< 0.001	1.007	1.006	1.009
GGN uniformity of density (heterogeneous vs. homogeneous)	< 0.001	2.151	1.587	2.915
Nodule-lung interface (not defined vs. well defined)	< 0.001	1.915	1.384	2.651
GGN with spiculation (yes vs. no)	< 0.001	2.097	1.519	2.896
GGN with vessel changes				
No	Reference	-	-	-
Type I	0.002	1.678	1.216	2.317
Type II	0.027	3.577	1.153	11.097
Type III	0.999	-	-	-

LUAD, lung adenocarcinoma; OR, odds ratio; CI, confidence interval; GGN, ground glass nodule; CT, computerized tomography. The invasion of lung adenocarcinoma by GGN features (ILAG) predictive model was described as follow: P=Exp [-1.098+0.323 (GGN diameter) + 0.007 (GGN CT attenuation) + 0.766 (GGN uniformity of density) + 0.650 (Nodule-lung interface) + 0.741 (GGN with spiculation) + 0.518 (GGN with Type I vessel changes) + 1.275 (GGN with Type II vessel changes) + 15.348 (GGN with Type III vessel changes)]/1 + Exp [-1.098+0.323 (GGN diameter) + 0.007 (GGN CT attenuation) + 0.766 (GGN uniformity of density) + 0.650 (Nodule-lung interface) + 0.741 (GGN with spiculation) + 0.518 (GGN with Type I vessel changes) + 1.275 (GGN with Type II vessel changes) + 15.348 (GGN with Type III vessel changes)].
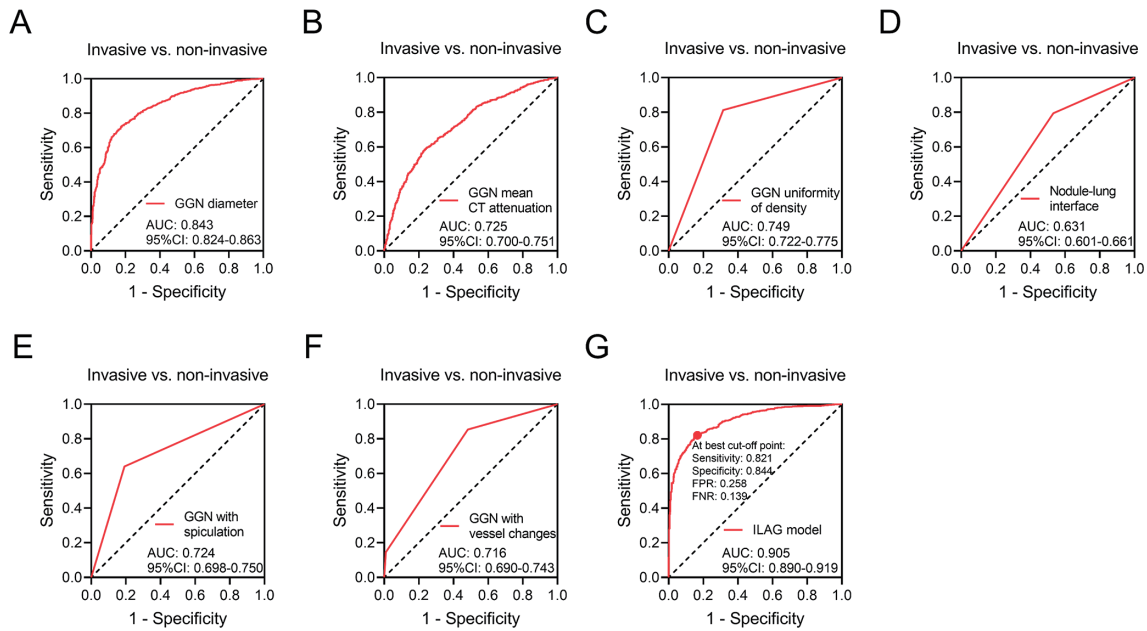
Fig. 1. The performance of ILAG model in distinguishing invasive LUAD from non-invasive LUAD.
The predictive values of GGN diameter (A), GGN mean CT attenuation (B), GGN uniformity of density (C), nodule-lung interface (D), GGN with spiculation (E), GGN with vessel changes (F), and the combination of these six independent GGN features (G) for invasive LUAD. LUAD, lung adenocarcinoma; GGN, ground-glass nodules; CT, computed tomography; AUC, area under curve; CI, confidence interval.

and IAC (Supplementary Table S2).

Discussion

LUAD is a rapidly fatal tumor with poor overall survival, and researches suggest that although there are multiple prognostic factors for LUAD, such as age, history of smoking and pathological grades, the most determinant factor for LUAD survival is the tumor invasiveness (Lee et al. 2013). The characteristics of GGN are shown to be indicative for the malignancy of the lesion, whereas for the correlation of GGN characteristics with the invasiveness of LUAD, only key characteristics of GGN have been studied. For instance, a study investigating the association of GGN and LUAD invasion reveals that the diameter and volume of nodule is strongly correlated with the invasiveness of LUAD (Wang et al. 2017). Other features such as mean CT attenuations, lesion borders (smooth or notched) and shape (round or oval) are reported to differentiate MIA from non-invasive subtypes (Wang et al. 2017). Although these GGN features are indicative for invasiveness of LUAD, there lacks a comprehensive screening of GGN features by HRCT, or the available studies focus on the features of a group of GGN rather than all susceptible GGNs. Therefore, in the present study, we comprehensively screened for the characteristics of GGN by HRCT in LUAD patients, and assessed the predictive value of these characteristics for LUAD invasiveness, aiming to construct a predictive model to accurately forecast the invasiveness of LUAD. From univariate logistic regression model, GGN features including distance from pleura (< 2 mm vs. ≥ 2 mm), diameter, area, mean CT attenuation, uniformity of density (heteroge-

neous vs. homogeneous), shape (irregular vs. round or oval), margin status (coarse vs. smooth), nodule-lung interface (not defined vs. well defined), with spiculation (yes vs. no), with pleural indentation (yes vs. no), with air bronchogram (yes vs. no), with vacuole sign (yes vs. no), with vessel changes (type I and type II vs. no), with lobulation (yes vs. no) were risk factors for invasive LUAD. Some of the features such as diameter and mean CT attenuation were consistent with the previous findings. This finding could be explained as follows: These GGNs with nearer distance from pleura, larger size, higher mean CT attenuation, heterogeneous uniformity of density, irregular shape, coarse margin status, not defined nodule-lung interface, spiculation, pleural indentation, air bronchogram, vacuole sign, vessel changes, lobulation might stand for the worse differentiation of lung cancer cells, therefore they contributed to invasive LUAD.

Although the predictive value of GGN features on invasive LUAD are shown, there still lack a systematic model/criterion that integrates the contribution of key GGN features for invasive LUAD prediction. Thus, as a step further, we conducted multivariate logistic regression analysis and disclosed six GGN features that independently contributed to invasive LUAD, which were GGN diameter, GGN mean CT attenuation, GGN uniformity of density, nodule-lung interface, GGN with spiculation, GGN with vessel changes. In addition, we constructed the systemic predictive model containing these six independent predictors (namely the ILAG predictive model) for determining invasive LUAD. The predictive value of these independent factors were shown to be relatively good as assessed by ROC

curve analysis, and the ILAG predictive model was illustrated to have excellent predictive value for invasive LUAD. Individually, the size of a nodule has been extensively reported to correlate with the invasiveness of LUAD, similarly, in our study, GGN diameter yielded an AUC value of 0.843 in distinguishing invasive LUAD from non-invasive LUAD (Lim et al. 2013). Besides, evidence shows that CT attenuation is negatively associated with retained air space that is increased in non-invasive tumors, therefore, higher CT attenuation correlates with invasive LUAD (Yang et al. 2001). As for the nodule density, homogenous and low density tends to indicate non-solid GGN, which are less invasive (Kitami et al. 2016), thus, the heterogeneous uniformity of density that are more likely to be solid, is correlated with invasive LUAD. Collectively, ILAG predictive model had better predictive value compared with the individual independent GGN features (presented by the higher AUC value), this was in accordance with one previous study that the combination of size and CT attenuation of GGN presented higher AUC compared with that of the individuals for predicting invasive LUAD (Eguchi et al. 2014). This indicated that ILAG predictive model might be a valuable predictive tool for invasive LUAD, and therefore assisting with LUAD management.

The limitations of this study included: (1) Only surgical LUAD patients were included, which might cause bias. (2) The assessment of GGN by different radiologists might vary, thus a uniformed criterion should be established if the ILAG predictive model was to be used in large scale. (3) The lack of a validation set was the main limitation of this study, which should be verified in further study.

In conclusion, the ILAG predictive model integrating GGN diameter, GGN mean CT attenuation, GGN uniformity of density, nodule-lung interface, GGN with spiculation, GGN with vessel changes by HRCT is potentially a useful approach for early estimation of LUAD invasiveness.

Funding

Conflict of Interest

The authors declare no conflict of interest.

References

Adams, S.J., Stone, E., Baldwin, D.R., Vliegenthart, R., Lee, P. & Fintelmann, F.J. (2023) Lung cancer screening. *Lancet*, **401**, 390-408.

Bai, C., Choi, C.M., Chu, C.M., Anantham, D., Chung-Man Ho, J., Khan, A.Z., Lee, J.M., Li, S.Y., Saenghirunvattana, S. & Yim, A. (2016) Evaluation of Pulmonary Nodules: Clinical Practice Consensus Guidelines for Asia. *Chest*, **150**, 877-893.

Chu, Z.G., Li, W.J., Fu, B.J. & Lv, F.J. (2020) CT Characteristics for Predicting Invasiveness in Pulmonary Pure Ground-Glass Nodules. *AJR Am. J. Roentgenol.*, **215**, 351-358.

Eguchi, T., Yoshizawa, A., Kawakami, S., Kumeda, H., Umesaki, T., Agatsuma, H., Sakaizawa, T., Tominaga, Y., Toishi, M.,

Hashizume, M., Shiina, T., Yoshida, K., Asaka, S., Matsushita, M. & Koizumi, T. (2014) Tumor size and computed tomography attenuation of pulmonary pure ground-glass nodules are useful for predicting pathological invasiveness. *PLoS One*, **9**, e97867.

Godoy, M.C.B., Lago, E.A.D., Pria, H., Shroff, G.S., Strange, C.D. & Truong, M.T. (2022) Pearls and Pitfalls in Lung Cancer CT Screening. *Semin. Ultrasound CT MR*, **43**, 246-256.

Gould, M.K., Donington, J., Lynch, W.R., Mazzone, P.J., Midthun, D.E., Naidich, D.P. & Wiener, R.S. (2013) Evaluation of individuals with pulmonary nodules: when is it lung cancer? Diagnosis and management of lung cancer, 3rd ed: American College of Chest Physicians evidence-based clinical practice guidelines. *Chest*, **143**, e93S-e120S.

Kitami, A., Sano, F., Hayashi, S., Suzuki, K., Uematsu, S., Kamio, Y., Suzuki, T., Kadokura, M., Omatsu, M. & Kunimura, T. (2016) Correlation between histological invasiveness and the computed tomography value in pure ground-glass nodules. *Surg. Today*, **46**, 593-598.

Lee, S.M., Park, C.M., Goo, J.M., Lee, H.J., Wi, J.Y. & Kang, C.H. (2013) Invasive pulmonary adenocarcinomas versus preinvasive lesions appearing as ground-glass nodules: differentiation by using CT features. *Radiology*, **268**, 265-273.

Liang, X., Zhang, C. & Ye, X. (2024) Overdiagnosis and overtreatment of ground-glass nodule-like lung cancer. *Asia Pac. J. Clin. Oncol.*, 1-7.

Lim, H.J., Ahn, S., Lee, K.S., Han, J., Shim, Y.M., Woo, S., Kim, J.H., Yie, M., Lee, H.Y. & Yi, C.A. (2013) Persistent pure ground-glass opacity lung nodules >/= 10 mm in diameter at CT scan: histopathologic comparisons and prognostic implications. *Chest*, **144**, 1291-1299.

Lung Cancer Medical Education Committee of the Chinese Medical Education, A., Lung Cancer Alliance of Chinese Thoracic, S., Society of Tumor Ablation Therapy of the Chinese Anti-Cancer, A., Tumor Ablation Expert Committee of the Chinese Society of Clinical, O. & Tumor Ablation Expert Group of the Chinese College of, I. (2024) Chinese expert consensus: multidisciplinary diagnosis and treatment of multiple ground-glass nodule like lung cancer (2024 edition). *Zhonghua Nei Ke Za Zhi*, **63**, 153-169.

Lv, X., Mao, Z., Sun, X. & Liu, B. (2023) Intratumoral Heterogeneity in Lung Cancer. *Cancers* (*Basel*), **15**, 2709.

MacMahon, H., Naidich, D.P., Goo, J.M., Lee, K.S., Leung, A. N.C., Mayo, J.R., Mehta, A.C., Ohno, Y., Powell, C.A., Prokop, M., Rubin, G.D., Schaefer-Prokop, C.M., Travis, W.D., Van Schil, P.E. & Bankier, A.A. (2017) Guidelines for Management of Incidental Pulmonary Nodules Detected on CT Images: From the Fleischner Society 2017. *Radiology*, **284**, 228-243.

Mangiameli, G., Cioffi, U. & Testori, A. (2022) Lung Cancer Treatment: From Tradition to Innovation. *Front. Oncol.*, **12**, 858242.

Mei, X., Wang, R., Yang, W., Qian, F., Ye, X., Zhu, L., Chen, Q., Han, B., Deyer, T., Zeng, J., Dong, X., Gao, W. & Fang, W. (2018) Predicting malignancy of pulmonary ground-glass nodules and their invasiveness by random forest. *J. Thorac. Dis.*, **10**, 458-463.

Ni, Y., Yang, Y., Zheng, D., Xie, Z., Huang, H. & Wang, W. (2020) The Invasiveness Classification of Ground-Glass Nodules Using 3D Attention Network and HRCT. *J. Digit. Imaging*, **33**, 1144-1154.

Sathish, G., Monavarshini, L.K., Sundaram, K., Subramanian, S. & Kannayiram, G. (2024) Immunotherapy for lung cancer. *Pathol. Res. Pract.*, **254**, 155104.

Shao, X., Shao, X., Niu, R., Xing, W. & Wang, Y. (2019) A simple prediction model using fluorodeoxyglucose-PET and high-resolution computed tomography for discrimination of invasive adenocarcinomas among solitary pulmonary ground-glass opacity nodules. *Nucl. Med. Commun.*, **40**, 1256-1262.

Travis, W.D., Brambilla, E., Nicholson, A.G., Yatabe, Y., Austin, J.H.M., Beasley, M.B., Chirieac, L.R., Dacic, S., Duhig, E., Flieder, D.B., Geisinger, K., Hirsch, F.R., Ishikawa, Y., Kerr, K.M., Noguchi, M., et al. (2015) The 2015 World Health Organization Classification of Lung Tumors: Impact of Genetic, Clinical and Radiologic Advances Since the 2004 Classification. *J. Thorac. Oncol.*, **10**, 1243-1260.

Travis, W.D., Brambilla, E., Noguchi, M., Nicholson, A.G., Geisinger, K.R., Yatabe, Y., Beer, D.G., Powell, C.A., Riely, G.J., Van Schil, P.E., Garg, K., Austin, J.H., Asamura, H., Rusch, V.W., Hirsch, F.R., et al. (2011) International association for the study of lung cancer/american thoracic society/european respiratory society international multidisciplinary classification of lung adenocarcinoma. *J. Thorac. Oncol.*, **6**, 244-285.

Udelsman, B.V. & Blasberg, J.D. (2023) Advances in Surgical Techniques for Lung Cancer. *Hematol. Oncol. Clin. North Am.*, **37**, 489-497.

Wang, H., Chen, A., Wang, K., Yang, H., Wen, W., Ren, Q., Chen, L., Xu, X. & Zhu, Q. (2024) CT imaging features of lung ground-glass nodule patients with upgraded intraoperative frozen pathology. *Discov. Oncol.*, **15**, 29.

Wang, X., Wang, L., Zhang, W., Zhao, H. & Li, F. (2017) Can we differentiate minimally invasive adenocarcinoma and non-invasive neoplasms based on high-resolution computed tomography features of pure ground glass nodules? *PLoS One*, **12**, e0180502.

Yang, Z.G., Sone, S., Takashima, S., Li, F., Honda, T., Maruyama, Y., Hasegawa, M. & Kawakami, S. (2001) High-resolution CT analysis of small peripheral lung adenocarcinomas revealed on screening helical CT. *AJR Am. J. Roentgenol.*, **176**, 1399-1407.

Zhang, Y., Shen, Y., Qiang, J.W., Ye, J.D., Zhang, J. & Zhao, R.Y. (2016) HRCT features distinguishing pre-invasive from invasive pulmonary adenocarcinomas appearing as ground-glass nodules. *Eur. Radiol.*, **26**, 2921-2928.

Supplementary Files

Please find supplementary file(s);
https://doi.org/10.1620/tjem.2024.J078